

LOW-EMITTANCE COMPACT RF ELECTRON GUN WITH A GRIDDED THERMIONIC CATHODE

T. Asaka[†], QST, Miyagi 980-8579, Japan

Abstract

A new type of rf electron gun has developed to generate a stable electron beam with a low-emittance of less than 2 mm mrad, that can be injected into Soft-x ray free electron laser (SX-FEL) and (Diffraction-limited storage ring) DLSR, without using a large ultraviolet laser system nor an ultra-high voltage pulsed. This electron gun consists of a 50 kV pulsed gun equipped with a commercially available thermionic cathode with grid and a 238-MHz acceleration cavity driven by a 42-kW solid-state amplifier. The system is simple, stable, robust, and easy-maintenance. To obtain a “grid-transparent” condition, the cathode voltage and the control grid voltage are optimized not to distort the electric field near the grid. To avoid the emittance growth due to the space charge effect, the gun and a special magnetic lens are embedded in the 238-MHz cavity at the shortest distance, and the beam energy is immediately accelerated to 500 keV. The first model of this electron gun has been operated as the 1 GeV injector of the NewSUBARU storage ring. The same electron gun will also be used in the injector linac of the 3 GeV light source under construction in Japan. This paper presents an overview of the rf electron gun system and our proof-of-performance experimental results.

INTRODUCTION

Gridded thermionic guns are used as electron sources for accelerator facilities because of their reliability, easy maintainability and long lifetime. Commercially available thermionic cathodes with a radius of 4 mm have a normalized emittance of larger than 10 mm mrad [1-4], but x-ray and soft x-ray free electron laser (XFEL and SXFEL) requires an order-of-magnitude smaller emittance of less than 2 mm mrad. The low-emittance electron sources developed for XFELs fall into two principal categories: photocathode radio-frequency (rf) guns [5, 6] and high voltage thermionic guns [7]. The photocathode rf guns have been used in many facilities as they provide a smaller and homogeneous emittance and have a more compact size. The photocathode however requires a complex drive laser system at ultraviolet wavelength, which demands laser specialists to maintain stable and reliable operations of the rf guns. The high voltage thermionic gun is nearly maintenance free, but it requires a high voltage pulse modulator to generate a microsecond 500 keV beam. In addition, an electromagnetic chopper system needs to be installed downstream of the gun not only to cut a short pulse of 1 ns from the microsecond beam, but also to preserve the low electron beam emittance [8].

As a third type of low-emittance electron gun, we developed an rf gun using a gridded cathode, which provides a

sufficiently small beam emittance with pulse length shorter than 0.7 ns and offers the prime advantage of the thermionic gun while not requiring the complex high voltage pulse modulator and chopper systems [9]. Our system features a 50-kV thermionic gun connected to a 238-MHz rf cavity in order to immediately increase the beam energy to 500 keV or even higher. This system uses a commercially available gridded cathode that provides an electron pulse shorter than 1 ns, which assures high capture efficiency for the subsequent rf acceleration cavity. The electron bunch from the present electron source will be compressed by velocity bunching system consisting of 476-MHz and S-band rf cavities and two magnetic bunch compressors, similarly to SACLA [8]. The bunched beam will be accelerated to 3 GeV by a C-band acceleration system. Our simulation study shows generation of 3 GeV electron beam with peak current greater than 2 kA and a normalized slice emittance below 2 mm mrad is feasible with our 3 GeV linear accelerator system design.

An initial concern about our schema was how to suppress the emittance growth that resulted from the distorted electric potential (lens effect) near the grid mesh next to cathode. The lens effect originates from a mismatch between grid and gun high voltages, which forms the unnecessary electric field to transversally kick the electrons passing the grid. The lens effect is considered to be controllable by adjusting the grid voltage to compensate the distortion of the electric potential given by a gun high voltage of 50 kV [10]. To confirm this approach, we used computer simulations to determine the optimum conditions for making the grid transparent for the extracted beam in terms of the achieving a small emittance value. Based on the simulation results, we designed an electron gun system with a gridded thermionic cathode and built a gun test stand to verify the beam performance.

LOW EMITTANCE BEAM GENERATION IN ELECTRON GUN

The electron gun system comprises a 50-kV electron gun with a gridded thermionic cathode, magnetic lens, a 238-MHz rf cavity, and a beam collimator. The gun generates low-energy, short-pulsed, and homogeneous cylindrical electron beams with an initial normalized emittance of about 1 mm mrad with optimum grid voltage. Then, an axially symmetric magnetic lens focuses the beam so as not to spread it widely over the minimized distance to the downstream rf cavity. The 238-MHz rf cavity immediately accelerates the extracted beam to 500 keV to suppress emittance growth. The collimator just after the cavity adjusts the beam charge depending on the purpose of injecting electron beams into a storage ring or driving FELs.

[†] asaka.takao@qst.go.jp

To generate a pulsed beam, we selected a commercially available gridded thermionic cathode, EIMAC Y845 produced by CPI Inc. The gun high voltage was configured to be 50 kV, a relatively low voltage that confers the following three advantages: (1) it relaxes voltage endurance conditions, enabling reliable operation of the high voltage charger in the air without requiring insulation oil; (2) it simplifies the driving power supply by allowing use of solid-state power devices and consequently making the power-supply compact; and (3) it reduces the grid voltage to a few hundred volts, which can be provided by such a commercially available pulse generator made by Kentech Instruments Ltd.

Theory of Cathode Emittance

We estimate the cathode emittance using the electron gun parameters listed in Table 1. The normalized rms thermal emittance is $\varepsilon_{n,T} = (r_b/2)(k_B T_C/mc^2)^{1/2} \approx 0.92 \text{ mm mrad}$, where $T_C = 1270 \text{ K}$ is the cathode temperature, k_B is the Boltzmann constant, m is the electron mass, and c is the speed of light. The magnetic emittance on the cathode is estimated to be $\varepsilon_{n,B} = eB_0 r_b^2/2mc \approx 0.23 \text{ mm mrad}$, where the magnetic field on the cathode from the geomagnetic field and other stay sources is assumed to be $B_0 = 0.5 \text{ G}$. The emittance growth due to the cathode surface roughness is estimated to be $\varepsilon_{n,R} = (\pi h)/(2l) r_b (eE_C h/(2mc^2))^{1/2} \approx 0.34 \text{ mm mrad}$ for $E_C = 1.2 \text{ MV/m}$, where $h = 1 \mu\text{m}$ is the amplitude of the surface roughness and $l = 20 \mu\text{m}$ is the period of the surface roughness. The cathode emittance is thus estimated to be $\sqrt{\varepsilon_{n,T}^2 + \varepsilon_{n,B}^2 + \varepsilon_{n,R}^2} = 1.0 \text{ mm mrad}$, satisfying the SXFEL requirement.

Table 1: Parameter of the Gridded Thermionic Gun

Parameter		Value
Cathode-anode voltage	Φ_A	50 kV
Cathode- anode gap	d	18 mm
Cathode-anode field	E_{CA}	-1.2 MV m ⁻¹
Cathode	C	Y845
Cathode radius	r_b	4 mm
Cathode temperature	T_C	1270 K
Cathode-grid gap	z_G	0.14 mm
Grid wire separation	$2a$	0.18 mm
Grid wire radius	r_0	0.01 mm

Emittance Growth due to Lens Effect

To preserve the initial small emittance, we optimized the mechanical and electrical parameters of the electron gun main components (such as the cathode, grid mesh and anode) so that the electric potential around the grid has a flat equipotential surface over the grid mesh as shown in Figure 1. This is an equivalent condition with the grid removed. The diagrams show the simulated electric field distributions around the grid and electron beam trajectories for various grid voltages. In the simulation, the gun high

voltages is fixed at 50 kV, while the grid voltage against the cathode is changed from 80 V to 240 V. As the grid voltage increases from 80 V, focusing electric field at the grid entrance decreases and the lens effect almost disappears at a grid voltage of 150 V, resulting in parallel beam trajectories after the grid. Since this grid-voltage optimization process limits flexibility to change the emission charge from the cathode, a round-shaped collimator was installed after the rf acceleration cavity to control the beam charge so as not to seriously degrade beam emittance.

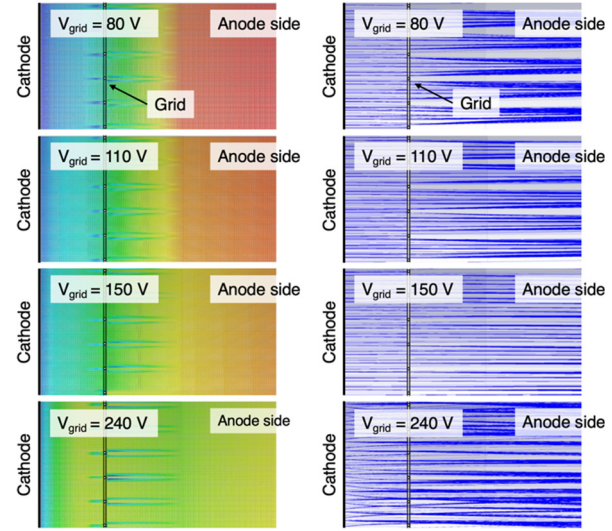


Figure 1: Electric field distribution (left) and beam trajectories (blue lines, right) near the grid of Y845 cathode obtained with CST simulations. The symbols V_{grid} represent the grid voltage and grid voltage conditions of 80, 110, 150, and 240 V, respectively. The color map shows the electric field the electric field strength (from blue at 0 MV/m to red at 1 MV/m).

DESIGN AND FABRICATION OF RF ELECTRON GUN SYSTEM

Simulation of 50-kV Gridded Thermionic Gun

Based on the consideration of the transparent grid scheme, we used CST simulations to design mechanical shape and arrangement of the 50-kV electron gun components such as Wehnelt and anode electrodes. The simulations optimize the focusing electric field which compensates for the defocusing by the electron beam space charge effect, enabling us to suppress the emittance growth from the initial thermal emittance and to maintain homogeneous beam distribution. The CST simulation takes into account the initial thermal emittance.

Figure 2 shows the beam aperture, arrangement, and mechanical shape for each component of the electron gun system. The Y845 cathode is composed of a cathode electrode and a grid mesh attached to the cathode with a gap of 0.14 mm. The diameters of the cathode and grid are 8 and 15 mm, respectively.

This gridded cathode is located 0.5 mm upstream from the entry of the Wehnelt electrode with a beam aperture of 13 mm in diameter. This aperture is smaller than that of the

grid, to slightly focus the beam as it exits the grid. The transverse beam size decreases smoothly as it moves downstream, due to a focusing electric field given by the Wehnelt with an opening angle of 52.5 degrees.

A parallel cylindrical beam with a diameter of 6 mm is obtained at the anode exit. The physical aperture of the anode electrode of 16 mm in diameter and its distance from the cathode surface are optimized to achieve a flat equipotential surface of the electric field over the transverse beam size. This optimization also results in a low electric-field strength of less than 8 MV/m at anode surface, which is sufficiently lower than the limit of electric discharge when -50 kV is applied to the cathode.

The simulation results for the transverse and horizontal phase space distributions are shown in Fig. 3, respectively. Table 2 summarizes the main parameters at the electron gun exit obtained with CST simulation. A normalized emittance of 1.3 mm mrad at a beam charge of 1 nC is predicted.

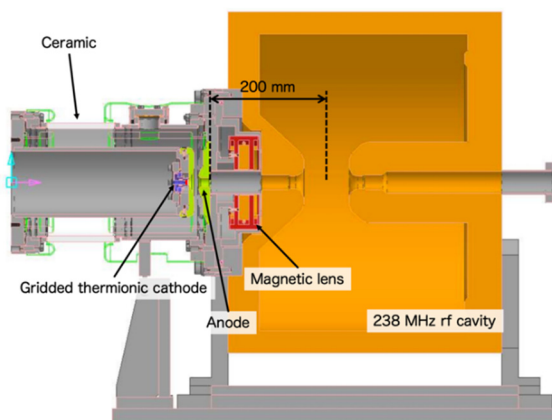


Figure 2: Beam aperture, arrangement, and mechanical shape of each component along the rf electron gun system.

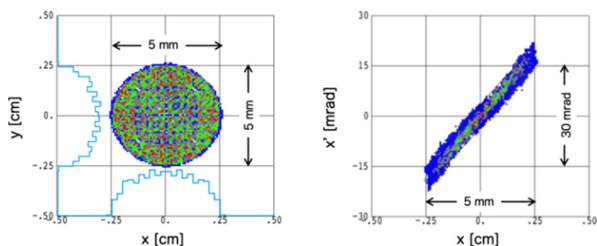


Figure 3: Particle distribution in the transverse (left) and horizontal phase space (right) at anode exit of the 50-kV electron gun with gridded thermionic cathode obtained with CST simulation.

Table 2: Beam Parameters at the 50-kV Electron Gun Exit

Parameter	Value
Energy	50 kV
Beam charge	1 nC (1.7 A / 600 ps)
Beam size	5 mm diameter
Normalized emittance	1.3 mm mrad

Simulation of Beam Transport and Acceleration

The phase space distributions at the 50-kV electron gun exit obtained with CST simulation are used as inputs for PARMELA simulation which is performed from the gun exit to a beam diagnostic system downstream the 238-MHz cavity. The solenoid field by the magnetic lens is adjusted so that the normalized emittance at the 238-MHz rf cavity is minimized without beam loss. The normalized emittance in the magnetic lens increases up to 2.5 mm mrad with a beam charge of 1 nC due to the space charge effect. The simulation demonstrates that the 60% core part of the extracted beam has a normalized emittance of 2.0 mm mrad with a beam charge of 0.6 nC. This indicates emittance growth from the initial thermal emittance of 0.93 mm mrad is small in the present gun system. The simulation results for the transverse and horizontal phase space distributions after the 238-MHz rf cavity exit are shown in Fig. 4, respectively.

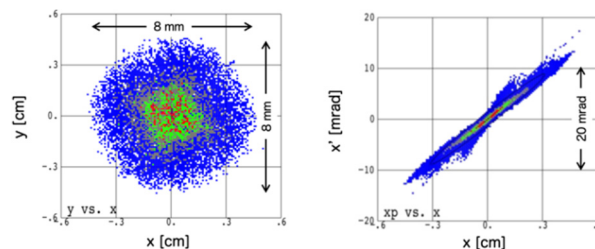


Figure 4: Particle distributions in the horizontal (left) and horizontal phase space (right) at the rf electron gun exit obtained with PARMELA simulation.

Magnetic Lens

Beam transport from the gun anode exit to the rf cavity entrance at the low energy of 50 keV potentially causes serious emittance growth due to the space charge force arising from static electric potential inside the electron beam itself. A shorter transport distance can alleviate the emittance growth due to the nonlinear space charge force which cannot be compensated by an emittance compensation solenoid.

Reduction of leakage field from the magnetic lens along the beam propagating direction is critically important to minimize the distance from the electron gun exit to the rf acceleration gap as well as to maintain sufficient field separation among three components of the present rf electron gun system (the 50-kV electron gun, the magnetic lens, and the rf cavity). For this purpose, we developed an axially symmetric magnetic lens shown in Fig. 5 (left figure) where the main solenoid coil has correction coils and soft iron yokes at both ends to reduce field leakage. Therefore, the magnetic field area is limited to 150 mm with this design, which is shown in Fig. 5 (right figure).

To embed the magnetic lens in the rf cavity, the magnetic lens is enclosed in a metal casing with two vacuum flanges. This built-in magnetic lens provides a vacuum beam pipe as shown in Figure 6. The distance from the anode exit of the electron gun to the center of the acceleration gap is shortened to 200 mm, as shown in Figure 2

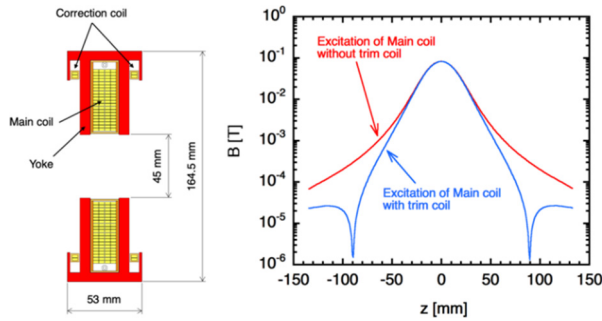


Figure 5: Cross section of the magnetic lens with the correction coils and yokes (left). Magnetic field distributions (right) with and without correction coil on the beam axis (blue and red solid lines).

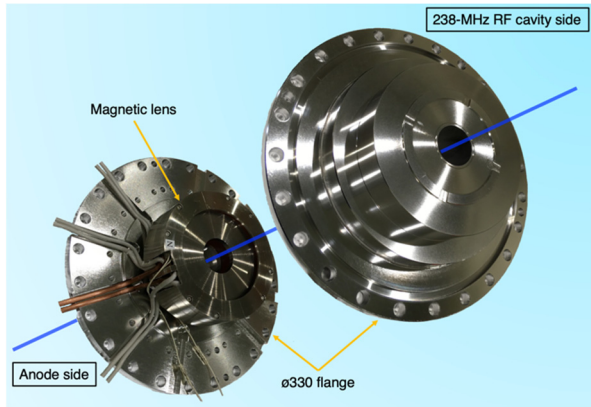


Figure 6: Metal casing enclosing the magnetic lens.

238-MHz RF Acceleration System

A 238-MHz rf cavity needs to satisfy the following condition: (1) a high field gradient to accelerate a 50 keV beam up to 500 keV which is equivalent to a shunt impedance of 6 M Ω for 34 kW input power; (2) a structure minimizing the beam transport distance from the anode exit to the rf cavity acceleration gap; (3) an axially symmetric acceleration field distribution.

The required high shunt impedance can be satisfied with a rf cavity structure using an acceleration gap with a narrow beam aperture. This is because the structure can provide a high and relatively uniform acceleration field in the beam aperture without increase of manufacturing costs. The only disadvantage is the narrow beam aperture which can be overcome by keeping the beam size small enough through the rf cavity. By using PARMELA simulation, the aperture of the rf cavity was finally determined to be 22 mm in diameter, which is about 3 times larger than the beam size of 6 mm in diameter, providing the relaxed alignment tolerance.

The acceleration gap is placed upstream of the 238-MHz rf cavity to minimize the beam transport distance. In addition, the rf cavity is designed to maintain electromagnetic field symmetry in the beam propagating region while symmetry breaking components such as an rf input coupler and frequency tuners need to be installed. We installed an input coupler and tuners at the downstream sidewall where the acceleration gap is not directly seen.

The 238-MHz rf cavity is driven by the solid-state amplifier with a peak power of 42 kW and a pulse duration of 100 μ s. This amplifier is composed of 36 power FETs, each of which provides rf power of 1.5 kW. All the rf pulses from 36 FETs are superimposed using a 36-way cavity-type combiner. The superimposed rf power is fed into the rf cavity through a 39D-type coaxial transmission line. This solid-state amplifier is compact in size and reliable in operations with low rf noise. Table 3 summarizes main parameters of the 238-MHz rf system.

Table 3: Main RF Parameters of the 238-MHz RF Acceleration System

Parameter	Design	Achieved
Resonant frequency	238 MHz	238 MHz ± 100 kHz
Q_0	25400	23000
Shunt impedance	6 M Ω	6.17 M Ω
rf input power	42 kW	42 kW
rf pulse width	100 μ s	100 μ s
Repetition rate	1 – 30 Hz	1 – 30 Hz

BEAM TEST

The Gun Test Stand for Proof of Performance

We built a gun test stand to demonstrate the beam performance of the rf electron gun. Figure 7 illustrates the gun test stand composed of a 50-kV electron gun, 238-MHz rf cavity, two additional magnetic lenses, and a beam diagnostic system to measure the beam charge, the beam energy, beam profile, and the projected transverse beam emittance at the exit of the rf electron gun system.

A 200 μ m-thick YAG:Ce screen is used to measure the beam profile in high spatial resolution. A random shutter CCD camera with a telecentric objective lens is used to measure the screen image over a size of ± 30 mm at a high spatial resolution of 31 μ m without distortion.

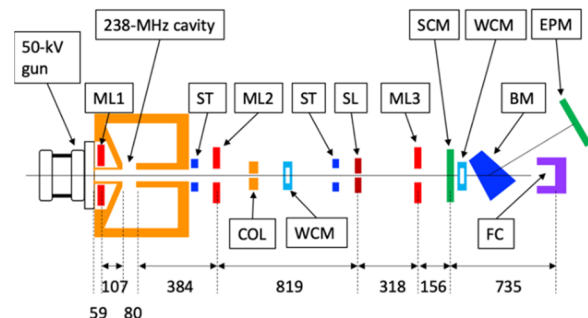


Figure 7: Layout of the gun test stand. The symbols ML, ST, COL, SL, WCM, FC, SCM, EPM, and BM represent a magnetic lens, a steering coil, a beam collimator, a beam slit, a wall current monitor, a Faraday cup, a screen monitor, an energy profile monitor, and a 30° bending magnet, respectively.

Measured Beam Performance

The beam charge was measured using a Faraday cup with a digital oscilloscope and set to be 1 nC for the

following measurements. The beam energy at the gun exit was derived from a time of flight (TOF) measurement between two wall current monitors. The energy resolution of the TOF method is estimated to be 2 % for 500 keV electron beam. Green points in Fig. 8 show measured beam energies as a function of the rf power fed into the 238-MHz rf cavity. The measurement agrees well with a calculation given by the blue solid line using the shunt impedance of 6.17 M Ω .

The projected horizontal emittance was measured by the slit scan method at a beam energy of 500 keV and a beam charge of 1 nC. The beam slit width of 100 μ m provides a charge low enough to suppress the beam divergence due to the space charge effect to a negligibly small level. Figure 9 shows the horizontal phase-space profile measured at a scan step of 250 μ m. A normalized horizontal emittance is evaluated to be 4.3 mm mrad in rms for a 90% core part of the whole electrons by subtracting the background noise from the image data. The normalized emittance decreases to 1.7 mm mrad in rms for a 60% core part of the whole electrons by cutting an additional 30% of the electrons with relatively large transverse momenta.

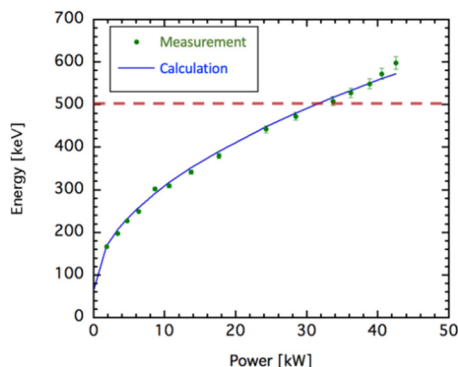


Figure 8: Beam energy dependence on the rf input power to the 238-MHz rf cavity. The green solid circles and blue solid line represent the measured data and calculation with a shunt impedance for the 238-MHz rf cavity, respectively.

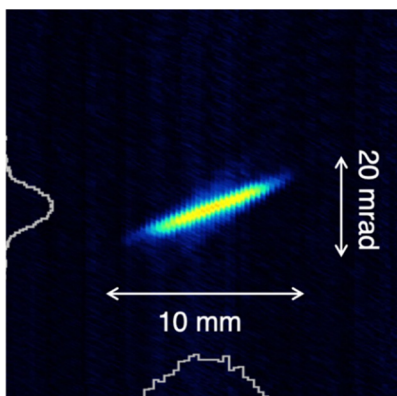


Figure 9: Measured phase-space profile of the 500 keV, 1 nC beam.

The normalized emittances measured at the slit position for beam energy of 500 keV are shown by blue solid line in Figure 10. The emittances are derived from the Gaussian fitting of the phase space distribution of the whole

electrons at each grid voltage to reduce the noise of the emittance measurement. A minimum emittance of 2.6 mm mrad is clearly observed for a 1-nC beam charge with peak current of 1.4 A around the grid voltage of 140 V.

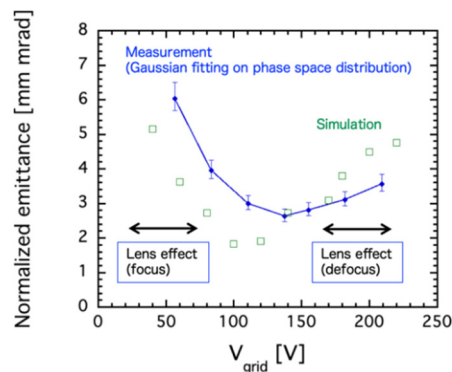


Figure 10: Normalized emittances at the slit for beam energy of 500 keV. Blue solid circles and green open squares are derived from the Gaussian fitting of the phase space distribution of the whole electrons for experiments and simulations, respectively.

CONCLUSION

We developed a low-emittance rf electron gun using a commercially available gridded thermionic cathode. Our proof-of-performance experiments agreed well with CST and PARMELA simulations: a normalized emittance of 1.7 mm mrad in rms for the 60% core part of the whole electrons at a beam energy of 500 keV and a beam charge of 1 nC. Since the projected normalized emittance can be reduced to a sufficiently the beam while keeping the beam charge more than 0.5 nC, our rf electron gun is a practical electron source for SFXEL systems.

REFERENCES

- [1] J. C. Bourdon *et al.*, “Commissioning the CLIO injection system”, *Nucl. Instrum. Methods Phys. Res., Sect. A*, vol. 304, pp. 322-328, 1991.
doi:10.1016/0168-9002(91)90878-T
- [2] R. J. Bakker *et al.*, “1 GHz modulation of a high-current electron gun”, *Nucl. Instrum. Methods Phys. Res., Sect. A*, vol. 307, pp. 543-552, 1991.
doi:10.1016/0168-9002(91)90229-J
- [3] T. Tomimasu *et al.*, “Strong focusing system of FELI 6-MeV electron injector used for ultraviolet range FEL oscillation”, *Nucl. Instrum. Methods Phys. Res., Sect. A*, vol. 407, pp. 370-373, 1998. doi:10.1016/S0168-9002(98)00052-7
- [4] N. Nishimori *et al.*, “A Thermionic Electron Gun System for the JAERI Superconducting FEL”, in *Proc. EPAC'00*, Vienna, Austria, Jun. 2000, paper MOP5A06, pp. 1672-1674.
- [5] X. J. Wang *et al.*, “Design and Construction a Full Copper Photocathode RF Gun”, in *Proc. PAC'93*, Washington, DC, USA, Mar. 1993, pp. 3000-3003.
- [6] R. Akre *et al.*, “Commissioning the Linac Coherent Light Source injector”, *Phys. Rev. Spec. Top. Accel Beams*, vol. 11, p. 030703, Mar. 2008.
doi:10.1103/PhysRevSTAB.11.030703

- [7] K. Togawa *et al.*, “CeB₆ electron gun for low-emittance injector”, *Phys. Rev. Spec. Top. Accel. Beams*, vol. 10, p. 020703, Feb. 2007.
doi: 10.1103/PhysRevSTAB.10.020703
- [8] T. Asaka *et al.*, “Low-emittance thermionic-gun-based injector for a compact free-electron laser”, *Phys. Rev. Accel. Beams*, vol. 20, p. 080702, Aug. 2017.
doi: 10.1103/PhysRevAccelBeams.20.080702
- [9] T. Asaka *et al.*, “Low-emittance radio-frequency electron gun using a gridded thermionic cathode”, *Phys. Rev. Accel. Beams*, vol. 23, p. 063401, Jun. 2020.
doi: 10.1103/PhysRevAccelBeams.23.063401
- [10] T. Asaka *et al.*, “Transparent-grid scheme for generating cathode-emittance-dominated beams in a gridded thermionic gun”, *Jpn. J. Appl. Phys.*, vol. 60, p. 017001, Dec. 2020. doi:10.35848/1347-4065/abd0c9